

## Research Article

Peter Fosodeder, Werner Baumgartner, Clemens Steinwender, Achim Walter Hassel, Camilo Florian, Jörn Bonse and Johannes Heitz\*

# Repellent rings at titanium cylinders against overgrowth by fibroblasts

<https://doi.org/10.1515/aot-2019-0070>

Received December 5, 2019; accepted March 24, 2020; previously published online May 1, 2020

**Abstract:** The invention of new miniaturized and smart medical implants continues in all medical fields, including miniaturized heart pacemakers. These implants often come with a titanium (Ti) casing, which may have to be removed after several months or years and shall therefore not be completely overgrown by cells or scar tissue after implantation. Scar tissue is mainly formed by fibroblast cells and extracellular matrix proteins like collagen produced by them. Suppression of fibroblast growth at Ti surfaces could be achieved by 800 nm femtosecond laser-ablation creating self-organized sharp spikes with dimensions in the 10  $\mu\text{m}$ -range which are superposed by fine sub- $\mu\text{m}$  parallel ripples. On flat Ti control samples, the best results regarding suppression of cell growth were obtained on spike-structures which were additionally electrochemically anodized under acidic conditions. When Ti cylinders with a diameter of 8 mm (similar as the pacemakers) were placed upright in a culture of murine fibroblasts, a multi-layer cell growth up to a height of at least 1.5 mm occurred within 19–22 days. We have demonstrated that a laser-structured and anodized ring around

the Ti cylinder surface is an effective way to create a barrier that murine fibroblasts were not able to overgrow within this time.

**Keywords:** cell-repellent surfaces; electrochemical treatment; femtosecond laser-processing; laser-induced micro- and nanostructures; medical implants.

## 1 Introduction

Controlled cell-adhesion on titanium (Ti) surfaces due to femtosecond-laser induced micro- and nanostructures have been investigated by several groups in the last years [1–3]. This interest is triggered by the fact that Ti and Ti-alloys are often used materials for medical implants, for instance in dentistry, orthopedics, and for cardio-vascular applications. The main focus up to now was the improved osseo-integration (e.g. the integration into the jaw bone for dental implants) due to the activation of bone-forming osteoblasts for enhanced production of bone material or the differentiation of mesenchymal stem cells into osteoblast cells, which can be induced by certain nano-features [4]. However, for many other applications the medical implants may have to be removed from the patient's body after certain period of months or years. In this case, a complete ingrowth into the tissue should be avoided. One example are the new miniaturized leadless intracardiac transcatheter pacing systems [5], marketed under the trademark Micra® (Medtronic plc, Dublin, Ireland). The advantage of this device over a traditional pacemaker system is the possibility to fully implant it into the right ventricle of the heart via the usage of a catheter. Four tines are used to fix the pacemaker to the myocardium, but the catheter can finally be removed again. If placed correctly, the average lifespan of the built-in battery allows the device to operate for 10–12 years, after which the device with the battery has to be exchanged again.

The design allows an explantation of the device also via catheter, by attaching a wire to the knob-like top end of the pacemaker and gently pulling out the tines,

\*Corresponding author: **Johannes Heitz**, Institute of Applied Physics, Johannes Kepler University Linz, Linz, Austria, e-mail: johannes.heitz@jku.at. <https://orcid.org/0000-0002-5608-5133>

**Peter Fosodeder:** Institute of Applied Physics, Johannes Kepler University Linz, Linz, Austria

**Werner Baumgartner:** Institute of Biomedical Mechatronics, Johannes Kepler University Linz, Linz, Austria

**Clemens Steinwender:** Department of Cardiology and Internal Intensive Medicine, Kepler University Hospital Linz, Linz, Austria

**Achim Walter Hassel:** Institute of Chemical Technology of Inorganic Materials, Johannes Kepler University Linz, Linz, Austria.

<https://orcid.org/0000-0002-9816-6740>

**Camilo Florian and Jörn Bonse:** Bundesanstalt für Materialforschung und -prüfung (BAM), Berlin, Germany. <https://orcid.org/0000-0003-4984-3896> (J. Bonse)

[www.degruyter.com/aot](http://www.degruyter.com/aot)

© 2020 THOSS Media and De Gruyter

 Open Access. © 2020 Johannes Heitz et al., published by De Gruyter.  This work is licensed under the Creative Commons Attribution 4.0 Public License.

ideally without harming the myocardium. However, a recent autopsy report [6] showed that major tissue growth around the device can occur. This led to the conclusion, that an explantation via catheter could not be possible anymore. In particular, multilayers of collagen were found to encapsulate the device. It was concluded that fibroblasts were responsible for the ingrowth of the pacing system. Therefore, ideas for preventing a full ingrowth of the device would be of large interest. Ranella et al. [7] have found that femtosecond laser-induced conical micrometer spikes and surface periodical nanometer ripples on silicon can be used to tune cell adhesion. It is assumed that the cells are not able to sufficiently adjust their shape to the micrometer surface structure, and therefore a limitation of the contact area between cell and substrate is achieved. Furthermore, the presence of nanometer sized periodic structures at the surface supposedly limits the amount of focal adhesions on the tips of the spikes. Additionally, electrochemical approaches for controlling the adsorption of certain extra cellular matrix proteins, such as collagen, on a titanium substrate have been found [8]. Our recent article by Heitz et al. [9] revealed that femtosecond-laser processing and subsequent electrochemical anodization of flat titanium surfaces can lead to a reduction of cell-substrate adhesion forces. As a consequence, it is supposed that a structured and subsequently electrochemically processed ring around the pacemaker would ideally act as a barrier for cells growing up from the bottom of the device. Hence, one could successfully prevent the ingrowth of the implant.

The state-of-the art is that cell growth on flat samples can be suppressed by laser-structuring their surface, as we and others have demonstrated for instance in refs. [7] and [9]. However, the growth mechanism of cells seeded homogeneously on a flat substrate is principally different from that of cells growing up on a three-dimensional structure which occurs from bottom to top. Therefore, the novelty of this work lies in the fact that we have demonstrated for the first time that an ultrafast-laser structured ring can stop cells from growing up on a cylindrical sample. This is relevant for important practical applications in the field of medical implants, for instance miniaturized pacemakers with cylindrical Ti-based casings attached to the inner heart wall. Here in particular, undesired ingrowth can occur by grow-up of the tissue from the heart wall up to the top of the implant.

In this work, we have combined and optimized femtosecond laser-structuring and electrochemical processing with respect to their capability of reducing cell adhesion on a cylindrical titanium sample. Subsequently, a processed ring around a cylindrical titanium sample, acting

as a barrier for further cell growth, is produced. By these measures, for instance the knob-like head of the pacemaker shall be kept free from cells in order to allow a safe explantation of the pacemaker, even after the full working period of the device.

## 2 Experimental

The experimental procedure described in this article is made up of three steps: femtosecond laser-structuring of titanium samples is followed by electrochemical oxidation (anodization) of the structured titanium samples and finally cell tests on structured and oxidized titanium samples are performed.

Samples cut from a Ti (3.7025) rod (Freude Titan GmbH & Co. KG, Sinsheim, Germany) with a similar diameter ( $\varnothing 8$  mm) as the pacemaker ( $\varnothing 7$  mm) were used for the experiments. For control experiments, flat Ti (3.7025) samples with an area of  $20 \times 20$  mm<sup>2</sup> were employed (Zapp Precision Metals GmbH, Schwerte, Germany). The laser-processing was done with an amplified femtosecond Ti:Sapphire laser system (Hurricane-1, Spectra Physics, Darmstadt, Germany) with a wavelength  $\lambda = 800$  nm, pulse duration  $\tau = 120$  fs, a typical pulse energy  $E = 50$   $\mu$ J, and a repetition rate of 1 kHz. Two linear stages were used for lateral movement. The cylindrical sample was mounted to a third stepper motor that is responsible for the rotation of the sample along its symmetry axis, as is shown schematically in the left part of Figure 1. The laser beam was focused with a lens (Thorlabs, Product ID: LB1945-B-ML) with focal length  $f = 200$  mm resulting in the Gaussian-shaped intensity profile with a beam diameter  $2\omega_0 \approx 52$   $\mu$ m at full width of half maximum (FWHM). The spatial beam profile was measured using a digital camera. The irradiation parameters (beam velocity 0.35 mm/s, line distance 10  $\mu$ m, average fluence 2.4 J/cm<sup>2</sup>) were optimized with the aim of achieving a regularly ordered surface structure consisting of 10–15  $\mu$ m spikes which were covered with laser-induced periodic surface structures (LIPSS, ripples) with a periodicity  $\Lambda \approx 350$  nm. Scanning electron microscope (SEM) images of the resulting surface structure are shown in Figure 1, as well, and in higher magnification in Figure 2 [with cross-sectional focused ion beam (FIB) cuts].

For anodization, a standard electrochemical cell as shown schematically in Figure 3 was used, where WE stands for working electrode, CE for counter electrode, and REF for reference electrode. The titanium sample was dipped into the electrolyte (0.1 M H<sub>2</sub>SO<sub>4</sub>, aerated), until the laser-structured ring was fully covered and left at open circuit polarization (OCP) for 100 s before electrochemical processing was started. For the reference electrode, Ag/AgCl in 3 M KCl was used [electrode potential 0.195 V vs. standard hydrogen electrode (SHE)], and for the counter electrode a gold wire (surface area ca. 7 cm<sup>2</sup>) was used. Additionally, the electrolyte was stirred by means of a magnetic plate. The anodization was performed during cyclic voltammetry (CV) with a voltage range  $U = 0$ –10 V and a scan rate of  $k_s = 0.1$  V/s.

To prove the functionality of the processed surface, cell tests using the murine fibroblast cell line LTK (ECACC, UK, catalogue no. 85011425) were performed. As a growth medium DMEM (Lactan, Graz, Austria) + 2 mM glutamine (Sigma) + 10% foetal calf serum (FCS, Biochrom, Berlin, Germany) + 50 U/ml penicillin + streptomycin (Serva, Heidelberg, Germany) was used. The cells were grown in

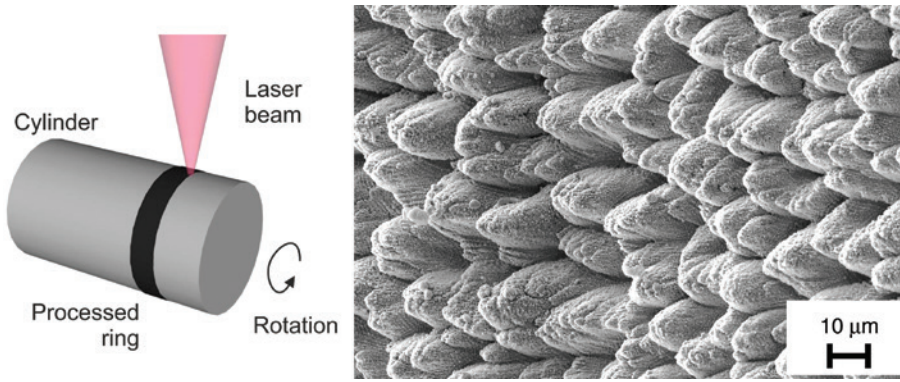


**Figure 1:** Structuring procedure (left): a focused femtosecond laser-beam irradiates a rotating Ti cylinder. The result is a structured ring; SEM image of the resulting structures (right): sharp micrometer spikes on the Ti surface are found covered with 350 nm period LIPSS.

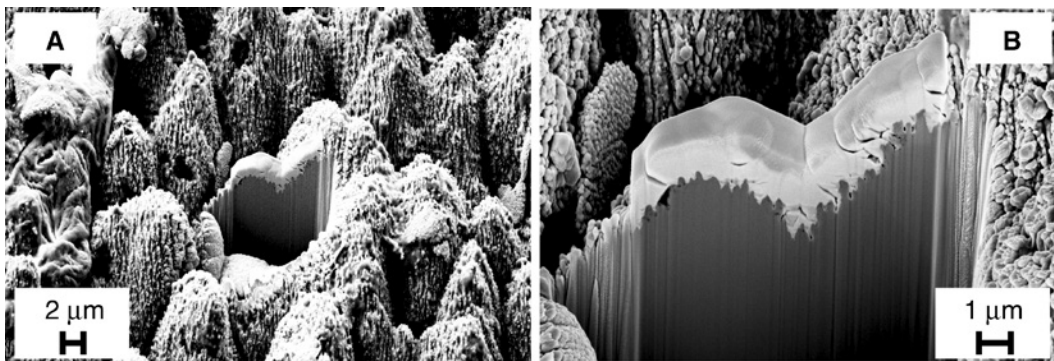


**Figure 2:** (A) High-magnification SEM image of femtosecond laser-induced spikes covered with sub-μm LIPSS with a FIB cut into one spike; (B) zoom-in into the FIB cut. The bright cover-layer on top of the spikes in the FIB-cutted region is a platinum surface protection layer.

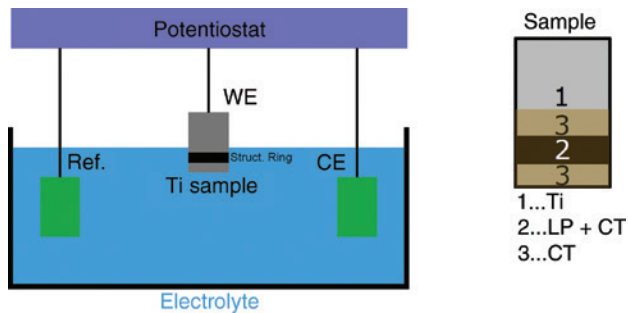


**Figure 3:** Electrochemical cell used for processing cylindrical samples: the titanium sample (WE) is dipped into the electrolyte (0.1 M  $\text{H}_2\text{SO}_4$ ) until the structured ring is fully covered (not true to scale). In total, three differently processed regions are created on the sample: (1) only titanium (Ti), (2) laser-processed and chemically treated (LP + CT), (3) only chemically treated (CT).

$\text{H}_2\text{O}$  saturated atmosphere with 5%  $\text{CO}_2$  at 37°C and were split once a week at a ratio of 1:10. The experiments with laser processed and chemically treated cylindrical samples were performed with seeding times between 19 and 22 days. Each set of differently treated samples (in total four sets of samples) was put in a Petri dish, together with two to four non-treated reference samples as illustrated in Figure 4. After fixation of the cells, the samples were sputter-coated with gold

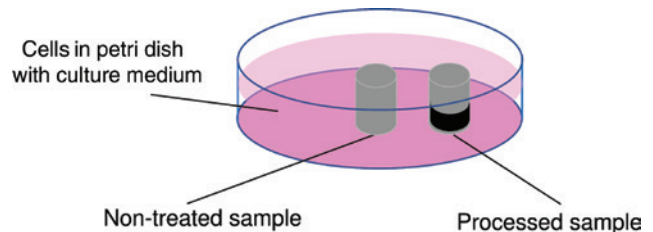


**Figure 4:** Cylindric samples in the Petri dish: the processed cylinders, together with the non-processed reference cylinders were uprightly placed in the Petri dish, with the structured ring covered by the cell-culture medium (pink).

and the resulting cell population on the sample was evaluated by means of an SEM.

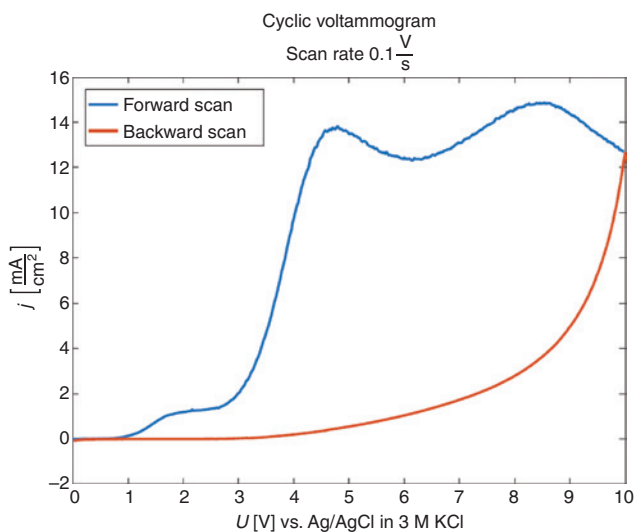
### 3 Results

Figure 2 shows a FIB cut of a femtosecond laser-induced spike. For technical reasons the flat samples were used for these images. The bright material on top of the FIB cut is a platinum cover layer, deposited locally before

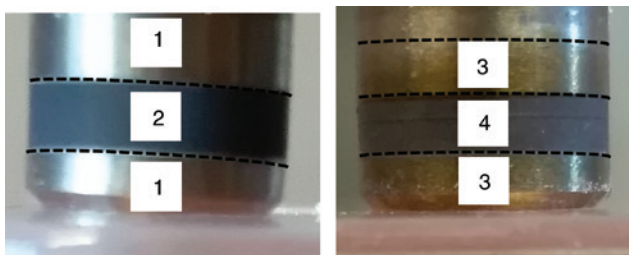
FIB cutting. While the height of the spikes is several  $\mu\text{m}$ , the LIPSS structures in Figure 2B have a height of about 150–200 nm, only. With the laser parameters used in this work, the LIPSS are no straight lines, but rather oriented chains of droplet-shaped nano-particles with some irregularities. Overall, the laser-induced structures have a pronounced hierarchical character of combined micro- and nano-features.

Figure 5 shows a cyclic voltammogram of a femtosecond laser-processed Ti cylinder. In the forward scan, the current density settles at about  $j=1.5 \text{ mA/cm}^2$  between  $U=1.5$  to 3.0 V. After exceeding the 3 V mark, a rapid increase in the current density up to  $j\approx 14 \text{ mA/cm}^2$  can be measured, followed by two oscillations of the current density until  $U=10 \text{ V}$  is reached. The backward scan shows a rapid decrease of the current density as soon as the voltage is reduced.

Figure 6 shows the optical appearance of a Ti cylinder with a femtosecond laser-processed ring without and with



**Figure 5:** Cyclic voltammogram of femtosecond laser-processed cylindrical Ti samples with the anodization parameters  $U=0$ –10 V and  $k_s=0.1 \text{ V/s}$ .



**Figure 6:** Cylindric Ti samples (left) only laser-processed, (right) additionally anodized: (1) non-treated Ti, (2) laser-structured ring at the Ti sample, (3) anodized Ti, (4) laser-structured and anodized Ti.

subsequent anodization. The non-treated Ti has a metallic shining appearance. The femtosecond laser-processed ring is black. Additional anodization under the conditions described in the ‘Experimental’ section, turns the color of the non-processed Ti into gold-brown and of the laser-processed ring into dark grey.

Femtosecond-laser processing in combination with electrochemical processing provides promising results in terms of cell repulsion. We have proved this idea previously in ref. [9] for fibroblasts on flat samples consisting of the Ti-alloy Ti6Al4V, containing about 6% Al and 4% V. Here, we have reproduced these effects with (very) pure Ti (3.7025) samples. The best repellence effect was achieved by combining the femtosecond laser-processing with electrochemical anodization with the parameters described in the ‘Experimental’ section.

Cylindric samples were laser-processed accordingly, anodized, and then seeded with fibroblasts with the same parameters and kept in culture for 19–22 days. Finally, the samples were characterized with a SEM. Simultaneously, non-treated reference samples were seeded for an equal time with each group of samples. Figure 7 represents the typical result of the cell growth on one reference sample and on one laser-processed and anodized sample. Several SEM images were merged together, in order to visualize cell growth in confluent layers from the bottom of the cylinder up to the structured ring for the laser-processed and anodized sample and higher than 1 mm for the reference sample.

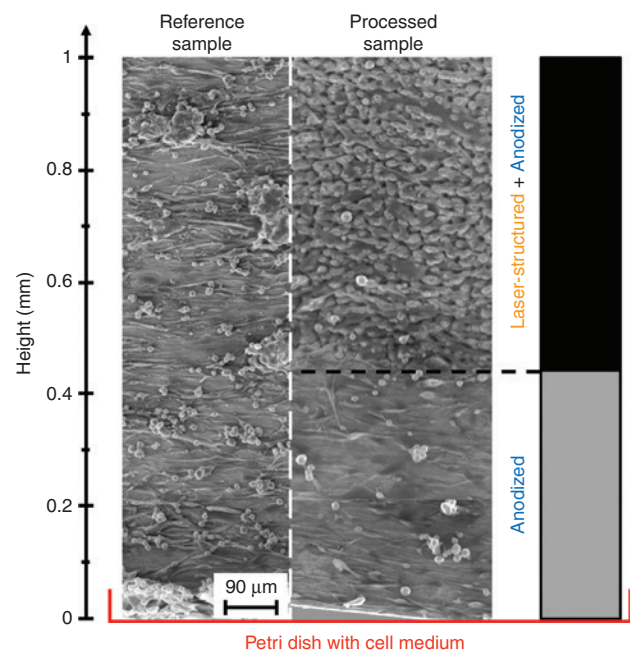


**Figure 7:** SEM images of cell growth on Ti cylinders (left) non-processed, (right) femtosecond laser-structured and anodized.

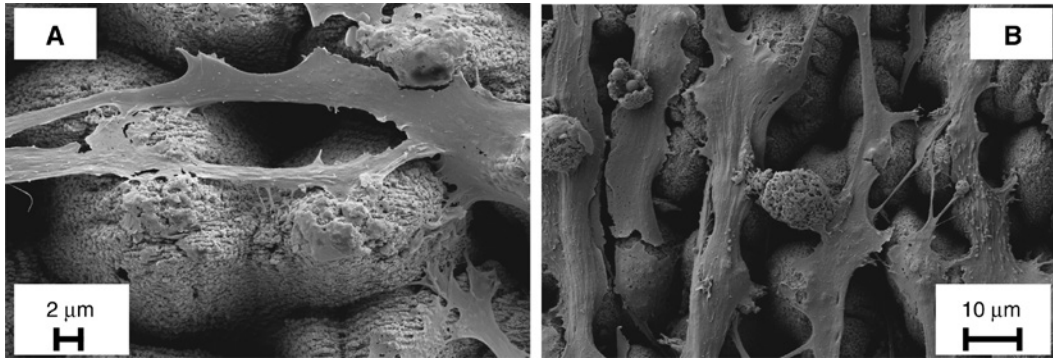


**Figure 8:** High-magnification SEM images of cells grown on femtosecond laser-structured and anodized Ti-cylinders: (A) few elongated cells; (B) several elongated and spherical cells.

As can be seen from Figure 8, it is easy to distinguish between the remaining few cells and laser-induced structures at higher SEM magnifications. Most of the cells are flat and elongated as the few cells in Figure 8A. These cells grow on top of the laser-induced structures not reaching into the valleys between the spikes. Most of the oriented cells follow the direction of the LIPSS structures. This also applies for Figure 8B which is rotated by  $90^\circ$  in comparison to Figure 8A. Besides the elongated cells, Figure 8B also shows some round features, which we interpret as cells which have lost the contact to the surface. We see spherical structures of different size, which may be either attributed to that in some cases there are cell fragments forming small spheres or that several cells agglomerate to one larger sphere.

## 4 Discussion

The first current density plateau at  $1.5 \text{ V} \leq U \leq 3 \text{ V}$  (see Figure 5) indicates a constant growth of new oxide. According to the high-field model [10], the ionic current, which is the source of oxide growth, should be constant also for larger applied voltages, therefore the first current density plateau can be identified as the ionic current. At  $U \approx 3.5 \text{ V}$  oxygen evolution [11] sets in, which can be observed in the form of  $\text{O}_2$  bubbles ascending in the electrolyte (especially from the laser-processed ring) and the fact that the current density rises rapidly. Oxygen evolution becomes possible, because the moving ions act as stepping stones for enhanced resonance tunneling. Oxygen vacancies in  $\text{TiO}_2$  lead to its n-type semiconductor behavior [12]. A definite reason for the second rise of the current density observed at  $U \approx 6 \text{ V}$  cannot be given here, but the relatively small changes are likely resulting from the rough electrode geometry and hydrodynamic effects of bubble formation

and release [13]. In the backward scan, the already formed oxide layer acts as a barrier for further oxidation. Therefore, the electrical field strength decreases and the possibility to overcome this barrier decreases rapidly until the current density drops to 0 again.

The black color of the laser-processed ring in Figure 6 is probably due to a light-trap effect of the sharp femtosecond-laser induced microstructures, similar as for ‘black silicon’ which was suggested for applications in photovoltaics and infrared optoelectronics [14]. Oxidized Ti surfaces are well known for their colorful appearance, which is often used for medical implants to guide the users. The brownish color of the regions (3) in Figure 6 can be attributed to oxide-layer thickness in the order of 100 nm [15, 16]. The effective thickness of the oxide-layer in femtosecond-laser and anodized area (4) is probably considerably larger [17], considering that the irradiation process takes place in air environment with a combination of (i) high energy deposited by the laser that increases strongly the sample surface temperature and (ii) an increase of the effective surface induced by the topography inherent of the spike structures. The latter effect is relevant as well for the laser-induced oxidation as for the electrochemical oxidation. The detailed analysis of the oxide-layer thickness and composition is a topic of our ongoing research effort.

Furthermore, we want to point out that no obvious modification of the nano-roughness of the laser-induced structures due to the anodization can be seen by means of SEM. This is corroborated, for instance, by a comparison of the cell free areas in Figure 8 (anodized) to the images in Figure 2 (not anodized), even though the additional oxidation due to the anodization certainly leads to changes of the morphology on the crystalline level. A detailed investigation of the nano-roughness would be however very challenging, as the aspect ratio of the structures is too high for AFM measurements. Optical methods (i.e. white light interferometry) gave no results as the structured surface

is black and reflects not enough light. Classical stylus profilometry failed as the nanostructures are too fine.

As is discussed in [9], the cell-repulsion of the structured and oxidized Ti-alloy surface may be explained by three different aspects in cell adhesion. The contact area is limited to the tips of the spikes, which considerably weakens the possible adhesion forces. The effect of sub- $\mu\text{m}$  LIPSS structures is likely to restrict the number of focal adhesions which are in contact with the ridges of the ripples leading also to weaker adsorption. In addition, forced unfavorable distances of the focal adhesions in the cell membrane may induce cell-internal signal pathways leading to a separation from the surface. The oxidation of the surface may additionally limit the adhesion of important adhesion-promoting proteins or promote the adhesion of adhesion-limiting proteins (as suggested in [8] for various proteins).

For the cell tests performed on processed cylindrical samples, it was particularly interesting, how far cells would grow up on the cylinder, in order to determine the necessary height, at which the 1 mm thick structured ring is placed. The structured ring was placed above a height of 0.5 mm (see Figure 7) and all reference samples show multi-layer cell growth of at least up to a height of 1.5 mm after 19–22 days. Therefore, a cell-free structured ring would indeed imply a cell repellent effect of the considered processed ring. Samples prepared with femtosecond laser-processing in combination with anodization (using the conditions described in the ‘Experimental’ section, which gave the best results regarding cell-repulsion for flat samples) show a nearly cell-free structured ring, while the only chemically treated area is still well covered with confluent cell layers. Furthermore, the orientation of the sub-micrometer ripples (LIPSS), which is horizontal in Figure 7, could successfully stimulate the few remaining cells at the laser processed area to wrap around the cylinder with their elongated side, instead of climbing up vertically. This effect has to be attributed to cell-alignment by the LIPSS structures which we have described already several years ago for LIPSS structures on polymers [18]. By this measure, the vertically spanned distance per cell on the structured ring could be minimized.

## 5 Conclusion

The major aim of this work was to expand the applicability of femtosecond laser-processing for cell-repulsion from flat samples to cylindrical samples. In particular, we aimed to process a ring around cylindrical samples that would ideally act as a barrier for upgrowing cells and stop cell growth at a given height. This was achieved in a two-step

process. First, we provided a basic proof of the ability of the fibroblast cells to grow upwards on a vertical non-processed titanium cylinder surface. For this purpose, the non-processed titanium cylinders were seeded with murine fibroblasts for 19–22 days. All samples showed confluent cell layers until up to a height of at least 1.5 mm, before the cell layers started to get thinner. Then we proceeded with experiments on processed Ti cylinders. They were laser processed beginning at a height of 0.5 mm and anodized with cyclic voltammetry. Consistent with the cell test results obtained from flat samples, the cell test results obtained with the cylindrical samples showed an excellent cell-repellent effect. To conclude, a new method for producing cell repellent surfaces on objects with cylindrical geometry, which applies for many medical implants for instance miniaturized pacemakers, is presented and the cell repellent properties of these surfaces were successfully proven in systematic series of cell tests.

**Acknowledgements:** The authors acknowledge the project CellFreeImplant. This project has received funding from the European Union’s Horizon 2020 research and innovation programme under grant agreement No 800832, Funder Id: <http://dx.doi.org/10.13039/100010661>.

**Author contributions:** P. Fosodeder performed the femtosecond laser-processing of the samples in the framework of his master thesis; C. Steinwender brought in the expertise on miniaturized pacemakers; W. Baumgartner performed the cell tests; A.W. Hassel. was responsible for the anodization; C. Florian performed femtosecond laser-processing of control samples and chemical characterization of femtosecond laser-irradiated Ti surfaces; J. Bonse provided the expertise for processing nano- and microstructures upon femtosecond-laser irradiation; J. Heitz wrote the manuscript and supervised the thesis of P.F.

## References

- [1] A. Cunha, O. F. Zouani, L. Plawinski, A. M. Botelho do Rego, A. Almeida, et al., *Nanomedicine* 10, 725–739 (2015).
- [2] V. Dumas, A. Guignandon, L. Vico, C. Mauclair, X. Zapata, et al., *Biomed. Mater.* 10, 055002 (2015).
- [3] C. Zwahr, A. Welle, T. Weingärtner, C. Heinemann, B. Kruppke, et al., *Adv. Eng. Mater.* 21, 1900639 (2019).
- [4] M. J. Dalby, N. Gadegaard, R. Tare, A. Andar, M. Riehle, et al., *Nat. Mater.* 6, 997 (2007).
- [5] D. Reynolds, G. Z. Duray, R. Omar, K. Soejima, P. Neuzil, et al., *New. Engl. J. Med.* 374, 533–541 (2016).
- [6] A. Kypta, H. Blessberger, J. Kammler, M. Lichtenauer, T. Lambert, et al., *Can. J. Cardiol.* 32, 1578.e1 (2016).

- [7] A. Ranella, M. Barberoglou, S. Bakogianni, C. Fotakis and E. Stratakis, *Acta Biomater.* 6, 2711–2720 (2010).
- [8] L. Richert, F. Variola, F. Rosei, J. D. Wuest and A. Nanci, *Surf. Sci.* 604, 1445–1451 (2010).
- [9] J. Heitz, C. Plamadeala, M. Muck, O. Armbruster, W. Baumgartner, et al., *Appl. Phys. A* 123, 734 (2017).
- [10] in ‘Encyclopedia of Electrochemistry. Volume 4. Corrosion and Oxide Films’, Ed. By M. Stratmann and G. Frankel (Wiley-VCH, Weinheim, 2003).
- [11] J. P. Kollender and A. W. Hassel, *ChemElectroChem* 4, 1846–1848 (2017).
- [12] N. Xiliang, Z. Shuping, M. Gloria and K. Sohlberg, *Int. J. Photoenergy* 2009, 294042 (2009).
- [13] A. W. Hassel, M. M. Lohrengel, *Electrochimica Acta* 40, 433 (1995).
- [14] P. G. Maloney, P. Smith, V. King, C. Billman, M. Winkler, et al., *Appl. Optics* 49, 1065–1068 (2010).
- [15] A. Revathi, A. Dalmau Borrás, A. Igual Muñoz, C. Richard and G. Manivasagam, *Mater. Sci. Eng. C* 48, 301 (2015).
- [16] S. A. Lone, M. Muck, P. Fosodeder, C. C. Mardare, C. Florian, et al., *Phys. Status Solidi A* (2020), published online, doi: 10.1002/pssa.201900838.
- [17] C. Florian, R. Wonneberger, A. Undisz, S. V. Kirner, K. Wasmuth, et al., *J. Bonse Appl. Phys. A* 126, 266 (2020).
- [18] E. Rebollar, I. Frischauf, M. Olbrich, T. Peterbauer, S. Hering, et al., *Biomaterials* 29, 1796 (2008).

#### Peter Fosodeder

Institute of Applied Physics, Johannes Kepler University Linz  
Linz, Austria

Peter Fosodeder received his Bachelor as well as Master in Technical Physics from the Johannes Kepler University Linz, Austria. The topic of his Master thesis, which he defended in November 2018, was ‘Laser-Structured and Anodized Surfaces on Medical Implants for Reduced Adhesion of Cells’. Since then he is working on a PhD thesis in the field of Terahertz spectroscopy at Recendt GmbH in Linz, Austria.

#### Werner Baumgartner

Institute of Biomedical Mechatronics, Johannes Kepler University  
Linz, Linz, Austria

Werner Baumgartner obtained his Dipl.-Ing. (MSc) and PhD degrees in Mechatronics and Biophysics from the Johannes Kepler University Linz, Austria, in 1995 and 1997, respectively. During his master and doctoral theses, he worked on stochastic methods in electrophysiology and microscopy as well as on mathematical methods in the investigation of ion channels. After a sabbatical at the Yale University in the USA, he became a postdoctoral fellow at the Institute of Anatomy and Cell Biology of the University of Würzburg, Germany in 1998, and 1 year later a senior researcher. He earned the Habilitation degree for cellular biophysics in 2002 from the University of Würzburg. In 2004 he became a full professor of cellular neurobiology at the Institute of Biology II of the RWTH Aachen, where he stayed till 2013. Since then he has been the head of the Institute of Biomedical Mechatronics at the Johannes Kepler University Linz, Austria. His research interests include the investigation of adhesion- and cell-recognition molecules, atomic force microscopy, theoretical biophysics and biomimetics.

#### Clemens Steinwender

Department of Cardiology and Internal Intensive Medicine  
Kepler University Hospital Linz, Linz, Austria

Clemens Steinwender studied Medicine at the Medical University of Vienna, Austria and obtained there also his Doctor of Medicine (MD) in 1996. He joined in 1999 the Linz General Hospital, which is now part of the Kepler University Hospital in Linz. He earned the Habilitation degree for cardiology in 2010 from the Paracelsus Medical University Salzburg, Austria. In 2013, he became head of the Department of Cardiology at the Linz General Hospital. In Dec. 2013, he implanted the worldwide first Micra<sup>®</sup> pacemaker system. Since then he treated far more than 100 patients. Clemens Steinwender has a very great experience in all techniques, which are necessary for the implantation of leadless pacemakers. He has an excellent relationship to the ‘Physiological Research Laboratories’ (PRL) of Medtronic in Minneapolis, USA, where the Micra<sup>®</sup> has been exclusively developed.

#### Achim Walter Hassel

Institute of Chemical Technology of Inorganic Materials, Johannes  
Kepler University Linz, Linz, Austria. <https://orcid.org/0000-0002-9816-6740>

Achim Walter Hassel studied Chemistry at the Heinrich Heine University in Düsseldorf, Germany and made his PhD about ultrathin valve metal oxide films. After a 2-year research stay at the University of Hokkaido in Sapporo, Japan (JSPS and AvH Fellow), he built up a research team on electrochemistry and corrosion at the Max Planck Institute for Iron Research in Düsseldorf. From 2007, he was scientific director of the International Research School for Surface and Interface Engineering in Advanced Materials. In July 2009, he moved as full professor to the Johannes Kepler University Linz, where he leads the Institute for Chemical Technology of Inorganic Materials. Achim W. Hassel had a large several-year Christian Doppler Laboratory on combinatorial oxide chemistry and has common activities with many industrial partners including producers of Ti-based implants.

#### Camilo Florian

Bundesanstalt für Materialforschung und -prüfung (BAM), Berlin  
Germany

Camilo Florian was between February 2019 and February 2020 PostDoc researcher at the Federal Institute for Materials Research and Testing (BAM) in Berlin, Germany, then he moved as postdoctoral research fellow to the Princeton University in Princeton, USA. He received in 2005 his Bachelor in Physics from the National Pedagogics University, Physics Department in Bogota, Colombia and in 2012 and in 2016 his Master in Physical Engineering and his PhD degree, respectively, from the University of Barcelona, Department of Applied Physics and Optics in Barcelona, Spain. During his PhD work he did research internships at the Italian Institute of Technology, NanoPhysics Department in Genoa, Italy and at the CNRS, Aix-Marseille University, Laser, Plasmas and Photonics Processes LP3 in Marseille, France. From 2016 to 2018 he was Postdoctoral Fellow in the Laser Processing Group at the Spanish National Research Council (CSIC) in Madrid, Spain.

#### Jörn Bonse

Bundesanstalt für Materialforschung und -prüfung (BAM), Berlin,  
Germany. <https://orcid.org/0000-0003-4984-3896>

Jörn Bonse is a staff scientist at the Federal Institute for Materials Research and Testing (BAM) in Berlin, Germany. His research

interests include the fundamentals and applications of laser-matter interaction, especially with respect to ultrashort laser pulses, laser-induced periodic nanostructures, time-resolved optical techniques, laser processes in photovoltaics, and optical phase change materials. He received a PhD degree in Physics from the Technical University of Berlin (Germany) in 2001, and a Diploma degree in Physics from the University of Hannover (Germany) in 1996. Dr. Bonse has occupied various research positions at institutions such as the Max-Born-Institute for Nonlinear Optics and Short Pulse Spectroscopy (MBI) in Berlin, the Spanish National Research Council (CSIC) in Madrid (Spain), and the Laser Zentrum Hannover (LZH) in Hannover. He was appointed as a senior laser application specialist at Newport's Spectra-Physics Lasers Division in Stahnsdorf, Germany.

**Johannes Heitz**

Institute of Applied Physics, Johannes Kepler University Linz, Linz, Austria, [johannes.heitz@jku.at](mailto:johannes.heitz@jku.at). <https://orcid.org/0000-0002-5608-5133>

Johannes Heitz is expert in the field of laser-matter interaction at surfaces including photo-induced nanopatterning and modification of polymer surfaces, and deposition of thin polymer films by laser-ablation. He studied Physics in Freiburg (Germany) until 1989. Since then he is employed at the Institute of Applied Physics at the Johannes Kepler University Linz (Dissertation 1993, Habilitation 1999). Since 1999 he is Associate Professor at the university in Linz. From Jan. 1995 he stayed for 1 year in Tsukuba, Japan as research fellow.